



DayCent-CUTE: A global sensitivity, auto-calibration, and uncertainty analysis tool for DayCent

Xiuying Wang^{a,*}, Jaehak Jeong^b, Seonggyu Park^b, Xuesong Zhang^c, Jungang Gao^b, Nélida E.Q. Silvero^a

^a Agoro Carbon Alliance, Tampa, FL, USA

^b Blackland Research and Extension Center, Texas A&M AgriLife Research, Temple, TX, USA

^c USDA-ARS Hydrology and Remote Sensing Laboratory, Beltsville, MD, USA

ARTICLE INFO

Keywords:

Soil organic carbon
Global sensitivity analysis
Uncertainty analysis
Auto-calibration
Ecosystem model

ABSTRACT

Soil organic carbon (SOC) is a crucial metric for mitigating greenhouse gas emissions and developing climate-smart agriculture. DayCent is widely used to simulate SOC dynamics and soil trace gas fluxes in various ecosystems. In this study, we developed DayCent-CUTE (auto-Calibration, sensitivity, and Uncertainty analysis ToolSet) for conducting global sensitivity analysis (GSA), auto-calibration, and uncertainty analysis for the model. The tool encompassed a pair of GSA methods and two distinct parameter optimization methods.

A collection of 30 field experiments, encompassing 212 combinations of management treatments and 581 SOC measurements, was divided into 18 sites for calibration and 12 sites for independent model evaluation. The posterior parameter distribution obtained from the auto-calibration process reduces the model bias and RMSE values, while the Nash-Sutcliffe efficiency and R^2 values showed improvements. The DayCent-CUTE proves to be an efficient and flexible tool that enhances the applications of the DayCent model.

1. Introduction

The concentration of greenhouse gases (GHGs), particularly atmospheric CO_2 , escalates due to human activities. Fossil fuel combustion, including the burning of coal, oil, and natural gas for energy production and transportation, is a significant contributor to CO_2 emissions. Additionally, agriculture plays a prominent role as the primary source of methane (CH_4) and nitrous oxide (N_2O) emissions (Byrne and Kiely, 2008). Biogeochemical models are increasingly used to advance GHG accounting systems by effectively capturing intricate biogeochemical processes. These models enable the examination of how land management practices influence GHG emissions and the dynamics of soil organic carbon (SOC) in ecosystems, soils, and climates where direct observations are limited and costly.

Various biogeochemical models have been developed and utilized to quantify GHG emissions and SOC stocks. Notable examples include DayCent (Del Grosso et al., 2005), DeNitrification-DeComposition (DNDC) (Li et al., 2000), Environmental Policy Impact Climate (EPIC) (Williams, 1995; Wang et al., 2005), and Agricultural Policy

Environmental eXtender (APEX) (Williams and Izaurrealde, 2006; Wang et al., 2006; Feng et al., 2015). These models provide mathematical representations of soil biogeochemical processes and allow comparisons of simulated results with real-world observations to test our comprehension.

The DayCent model (Del Grosso et al., 2001) is a daily time-step version of the CENTURY model (Parton et al., 1994) and explicitly accounts for processes that generate N_2O , NO_x , and N_2 emissions, such as nitrification and denitrification. It has been extensively utilized to simulate soil organic matter (SOM) dynamics, N_2O and CH_4 fluxes, and estimate net CO_2 , N_2O , and CH_4 emissions from soils in the US national greenhouse gas inventory submitted by the US EPA to the UN Framework Convention on Climate Change. This involves an annual set of simulations covering GHG emissions from the majority of agricultural land use for the EPA annual report (USEPA, 2020), which requires model parameterization for standard crops, in addition to millions of model runs to estimate model uncertainty (Ogle et al., 2007, 2010; Del Grosso et al., 2010). Furthermore, DayCent is incorporated within the COMET-Farm¹ platform that implements the USDA's entity-scale greenhouse

* Corresponding author.

E-mail address: susan.wang@agorocarbon.com (X. Wang).

¹ <https://comet-farm.com>, accessed on 12/19/2022.

gas inventory methods (Powers et al., 2014).

While DayCent is a powerful tool for studying ecosystem dynamics, it requires expertise and resources to utilize and interpret its outputs effectively. One challenge in using DayCent is its extensive parameterization, where a sensitivity analysis is typically performed to identify the most influential parameters for subsequent calibration. Although DayCent calibration guidelines have been provided (Del Grosso et al., 2011), manual calibration is subjective and may not always produce optimal parameter estimates, resulting in considerable uncertainty. To address this, automatic calibration methods have been employed, such as utilizing parameter estimation software like PEST (Rafique et al., 2014) and Bayesian approaches (Gurung et al., 2020; Mathers et al., 2023). However, limited efforts have been made to develop a comprehensive tool for conducting GSA, auto-calibration, and uncertainty analysis for the model. To address this gap, our study focuses on developing and applying the DayCent-CUTE (auto-Calibration, sensitivity, and Uncertainty analysis ToolSet), which serves as a user-friendly GSA, calibration, and uncertainty analysis tool for DayCent.

Another challenge in using DayCent is the spin-up process, where the model is run for an extended duration, spanning several thousand years, using historical weather data, edaphic characteristics, and native vegetation to achieve a steady-state condition. The second simulation period, the base history, is then used to simulate the historical cropping or grazing practices before the time frame of most interest to the user (Hartman et al., 2021). However, studies have suggested that relying solely on initialization to equilibrium conditions may not provide accurate initial levels of SOC for process-based model simulations (Carvalho et al., 2008; Wutzler and Reichstein, 2007). Alternative methods for initializing SOC pools have been explored, such as relating conceptual carbon pools with measurable fractions of SOC based on soil physiochemical properties (Christensen 1996; Luo et al., 2016). Several biotic and abiotic properties control SOC storage and can serve as indicators for estimating initial SOC values (Wiesmeier et al., 2019). However, it is essential to acknowledge that accurately matching the conceptual pools with these measurable C fractions poses certain limitations, as noted by Dangal et al. (2022). Dangal et al. (2022) used a combination of diffuse reflectance spectroscopy and machine learning to relate the DayCent model's active, slow, and passive C pools with measurable particulate-, mineral associated-, and pyrogenic-forms of C fractions. They pointed out there is still a need for more measured data on C fractions to improve these methods. On the other hand, the U.S. Soil Enrichment Protocol (Climate Action Reserve, 2022) requires a C simulation model to use direct measures of SOC to initiate with-practice and baseline simulations for carbon crediting programs, highlighting the need for continued development of new ways to initialize SOC pools.

In light of these challenges, our study aims to achieve the following objectives: (1) develop a graphical user interface tool for conducting GSA, auto-calibration, and uncertainty analysis for the DayCent model; (2) assess the suitability of the EPIC approach (Williams, 1995) for initializing SOC pools in the DayCent model; and (3) illustrate the effectiveness of the DayCent-CUTE tool for GSA and auto-calibration by utilizing 30 experimental field studies to calibrate and validate SOC under different cropland management practices.

2. Material and methods

2.1. The DayCent model

DayCent is a process-based ecosystem biogeochemical model that simulates C and N dynamics, phosphorus and sulfur cycling, and the emissions of N₂O and CH₄ (Parton et al., 2001; Del Grosso et al., 2006, 2011). The model simulates various processes involved in ecosystem dynamics, including plant growth processes such as photosynthesis, phenology (timing of biological events), dry matter allocation, and senescence (aging and deterioration of plant material). It considers the soil water balance, soil temperature, and SOM dynamics.

In the current DayCent version, the DDCentEVI version² (EVI signifies a version of DayCent with the option to use Enhanced Vegetation Index, known as EVI data), the simulation of SOM focuses specifically on the top 30 cm soil layer. The SOM is categorized into active, slow, and passive pools. These pools represent different rates of C turnover and dynamics, aiming to simplify and capture the complex processes within the soil C cycle. The active and slow organic matter pools consist of both surface and soil components, while the passive pool is solely represented in the soil. The passive pool represents a relatively stable fraction of organic matter that decomposes slower than the active and slow pools. By dividing C into these pools, the model can simulate the transfer of C, organic matter decomposition, and the gradual accumulation or depletion of C over time. This division provides a more detailed depiction of C dynamics than using a single aggregate value for SOC. To account for organic matter inputs, plant materials such as plant residues and roots are transferred into these SOM pools from above and belowground litter pools (metabolic and structural) as well as three dead wood pools when using tree growth submodule. The DayCent model incorporates a comprehensive representation of organic matter inputs by considering the transfer of plant materials from above and belowground litter pools, as well as direct decomposition of dead wood into the active and slow pools. This approach enables a more accurate simulation of soil carbon dynamics and decomposition processes.

The model also considers mineral N transformations, including N₂, N₂O and NO_x emissions. The required inputs for the DayCent model include daily maximum and minimum temperature and precipitation, soil texture, land use, and land management information, such as crop planting and harvest dates, fertilization, irrigation, cultivation/tillage, grazing, and burning. The DayCent model's user manual and a detailed model description are provided by Hartman et al. (2021).

2.2. SOC initialization

DayCent has options for using Burke's equations and user-supplied initial values to initialize soil C pools. The standard approach is to perform a "spin-up" of the model for thousands of years under native vegetation and site-specific climate and soil conditions (Hartman et al., 2021; Dangal et al., 2022). This study introduces a new option for initializing soil C pools in DayCent, which involves using an exponential curve and two parameters from the EPIC model (Williams, 1995). Direct measurement of SOC and parameter tuning for soil C pool initialization have been applied in various models such as EPIC (Wang et al., 2005), APEX (Wang et al., 2006, 2012), and SWAT-C (Zhang et al., 2013). EPIC and APEX typically assume that the passive C pool makes up 40–70% of the SOC, and the active C pool is set at a default value of 4% (Izaurrealde et al., 2012). The fraction of the passive humus pool (FHP) in the plow layer of SOC is affected by the number of years the soil has been under cultivation.

$$\text{FHP} = 0.7 - 0.3 \times \text{EXP}(-0.0227 \times \text{YR}_c) \quad (1)$$

where YR_c is the number of years the soil has been cultivated. Eq. (1) sets the range of the FHP parameter between 0.4 and 0.7. The amounts of SOC in the active pool (SOC_{active}) and passive pool (SOC_{passive}) are estimated by:

$$\text{SOC}_{\text{active}} = \text{FBM} \times \text{SOC}_{\text{meas}} \quad (2)$$

$$\text{SOC}_{\text{passive}} = \text{FHP} \times (\text{SOC}_{\text{meas}} - \text{SOC}_{\text{active}}) \quad (3)$$

where FBM is a coefficient representing the fraction of SOC in the active C pool and ranges between 0.03 and 0.05; SOC_{meas} is the measured SOC for the 0–30 cm soil layer. The initial value of the slow C pool (SOC_{slow}) is the difference between SOC_{meas} and the sum of active and passive

² Copyright 2022 Colorado State University, Fort Collins, CO 80523 USA.

pools. During biomass decomposition, while soil microbial activities remove C, the losses of N can occur through plant uptake, leaching, nitrification, and denitrification,. The C:N ratio is typically around 10–12 (Allison, 1973; Halvorson et al., 2009).

2.3. DayCent-CUTE

The DayCent auto-Calibration, sensitivity, and Uncertainty analysis ToolSet (DayCent-CUTE) is a standalone desktop application with a Graphic User Interface (GUI) based on Python 3.9. The source code was adapted from the framework of APEX-CUTE (Wang et al., 2014). The GUI is designed with the Qt Designer tool in PyQt 5.³ DayCent-CUTE provides the flexibility to evaluate more than 50 model parameters of the DayCent model (Table 1) with two global sensitivity analysis (GSA) methods: (1) the extended Fourier amplitude sensitivity test (FAST) method (Saltelli et al., 2010) and (2) Sobol (Sobol, 2001; Saltelli et al., 2010). Both are variance-based GSA methods that estimate each parameter’s fractional contribution to the model output’s total variance. These variance-based methods involve a decomposition of the variance into components because of interactions (Helton and Davis, 2003). The FAST method uses a periodic sampling approach and a Fourier transformation techniques to decompose a variance of a model output into variances contributed by model parameters. The Sobol method uses low-discrepancy sequences for parameter sampling and estimation of sensitivity indices. As a result, the FAST method provides computational efficiency as an advantage over the Sobol method. However, the Sobol method is known for its robustness and is often used as a benchmark GSA method. The total effect index, S_{Ti} , or the total sensitivity index is calculated as (Saltelli et al., 2000):

$$S_{Ti} = \frac{E_{X_{-i}}(V_{X_{-i}}(Y|X_{-i}))}{V(Y)} = 1 - \frac{V_{X_{-i}}(E_{X_i}(Y|X_{-i}))}{V(Y)} \quad (4)$$

where X_i represents the parameter under evaluation for its sensitivity, X_{-i} denotes all other parameters excluding X_i , Y is the generic scalar model output equal to $Y = f(X_1, X_2, \dots, X_k)$, $V_{X_{-i}}$ is the variance of argument taken over X_i , $E_{X_{-i}}$ is the mean of argument taken over X_i . The Sobol total sensitivity index S_{Ti} measures the overall effects of fractional parameter interactions on the output variance in the full range of parameter space.

$$S_{Ti} = S_i + S_{ij}(i \neq j) + \dots + S_{1\dots i\dots s} \quad (5)$$

$$S_i = \frac{D_i}{D} \quad (6)$$

where S_i measures the first-order sensitivity of the i_{th} parameter; D is the sum of the model output variance (D_i). While conducting multi-sites GSA, our approach involved utilizing Kernel Density Estimation (KDE) to derive the probability density function of the S_{Ti} across different sites and we used the means of S_{Ti} values across the experimental sites to rank the parameter importance.

DayCent-CUTE incorporates two autocalibration techniques for the DayCent model: the Dynamically Dimensioned Search (DDS) algorithm (Tolson and Shoemaker, 2007; Yen et al., 2014) and the Shuffled Complex Evolution algorithm - University of Arizona (SCE-UA) (Duan et al., 1993). The DDS algorithm is developed as a parameter search method for complex watershed models needing optimization of multiple parameters. It uses a random perturbation that is dynamically adjusted by changing the dimension of the search using the scalar neighborhood size perturbation parameter, which allows the algorithm to escape regions around poor local minima in the parameter space. As a stochastic neighborhood search algorithm, it searches globally at the beginning and then dynamically and probabilistically, reducing the number of

Table 1
DayCent parameters available in DayCent-CUTE.

| Model parameter | Description | Initial value | Lower bound | Upper bound |
|-----------------|--|---------------|-------------|-------------|
| ANEREF(1) | The ratio of rain/potential evapotranspiration below which there is no negative impact of anaerobic soil conditions on decomposition | 1.5 | 1 | 2 |
| ANEREF(2) | The ratio of rain/potential evapotranspiration above which there is the maximum negative impact of anaerobic soil conditions on decomposition | 3 | 2.8 | 5 |
| ANEREF(3) | The minimum value of the impact of anaerobic soil conditions on decomposition; functions as a multiplier for the maximum decomposition rate. | 1 | 0.1 | 1.1 |
| DAMR(1,1) | Fraction of surface N absorbed by residue | 0.02 | 0.002 | 0.3 |
| DAMRMN(1) | Minimum C/N ratio allowed in residue after direct absorption | 15 | 5 | 30 |
| DEC1(1) | The maximum decomposition rate of surface structural litter, strucc(1) | 3.9 | 3 | 5 |
| DEC1(2) | Maximum decomposition rate of soil structural litter, strucc(2) | 4.9 | 3 | 7 |
| DEC2(1) | Maximum decomposition rate of surface metabolic litter, metabc(1) | 14.8 | 12 | 18 |
| DEC2(2) | Maximum decomposition rate of soil metabolic litter, metabc(2) | 18.5 | 16 | 21 |
| DEC3(1) | Maximum decomposition rate of surface active organic matter, som1c(1) | 6 | 4 | 8 |
| DEC3(2) | Maximum decomposition rate of soil active organic matter, som1c(2) | 7.3 | 5 | 10 |
| DEC4 | Maximum decomposition rate of soil passive organic matter, som3c | 0.0022 | 0.001 | 0.005 |
| DEC5(2) | Maximum decomposition rate of soil slow organic matter; som2c(2) | 0.12 | 0.05 | 0.25 |
| FAVAIL(1) | Fraction of N available per day to plants | 0.15 | 0.1 | 0.5 |
| FLEACH(1) | Intercept value for a normal day to compute the fraction of mineral N, P, and S which will leach to the next layer when there is a saturated water flow; normal leaching is a function of sand content | 0.5 | 0.001 | 1 |
| FLEACH(2) | Slope value for a normal day to compute the fraction of mineral N, P, and S which will leach to the next layer when there is a saturated water flow; normal leaching is a function of sand content | 0.05 | 0.001 | 0.5 |
| FLEACH(3) | Leaching fraction multiplier for N to compute the fraction of mineral N which leaches to the next layer when there is a saturated water flow; normal leaching is a function of sand content | 1 | 0.2 | 2 |
| FWLOSS(1) | Scaling factor for interception and | 1 | 0.2 | 2 |

(continued on next page)

³ <https://pypi.org/project/PyQt5>; last accessed on January 17, 2023.

Table 1 (continued)

| Model parameter | Description | Initial value | Lower bound | Upper bound |
|-----------------|---|---------------|-------------|-------------|
| FWLOSS(2) | evaporation of precipitation by live and standing dead biomass | 1 | 0.2 | 2 |
| FWLOSS(3) | Scaling factor for bare soil evaporation of precipitation | 1 | 0.2 | 2 |
| FWLOSS(4) | Scaling factor for transpiration water loss | 0.75 | 0.2 | 2 |
| OMLECH(1) | Scaling factor for potential evapotranspiration | 0.03 | 0.000001 | 1 |
| OMLECH(2) | Intercept for the effect of sand on leaching of organic compounds | 0.12 | 0.02 | 0.8 |
| OMLECH(3) | Slope for the effect of sand on leaching of organic compounds | 1.9 | 0.02 | 2 |
| P1CO2A(2) | Amount of water that needs to flow out of water layer 2 to produce leaching of organics | 0.17 | 0.1 | 0.25 |
| P1CO2B(2) | Intercept for sand controlling C loss as CO ₂ during decomposition from active pool | 0.68 | 0.55 | 0.74 |
| P2CO2(2) | Slope for sand controlling C loss as CO ₂ during decomposition from active pool | 0.55 | 0.3 | 0.8 |
| P3CO2 | Fraction of C loss as CO ₂ during decomposition from slow pool | 0.55 | 0.5 | 0.9 |
| PABRES | Fraction of C loss as CO ₂ during decomposition from passive pool | 100 | 70 | 200 |
| PEFTXA | Amount of residue which will give maximum direct absorption of N | 0.2 | 0.1 | 0.7 |
| PEFTXB | Intercept parameter for regression equation to compute the effect of soil texture on the microbe decomposition rate (the effect of texture when there is no sand in the soil). See e _{text} calculation in prelim.f. The factor e _{text} is used in somdec.f and affects the flow out of som1c(2) | 0.4 | 0.2 | 1.5 |
| PMCO2(2) | Slope parameter for regression equation to compute the effect of soil texture on microbe decomposition rate; the slope is multiplied by the sand content fraction. See e _{text} calculation in prelim.f. The factor e _{text} is used in somdec.f and affects the flow out of som1c(2) | 0.55 | 0.35 | 0.65 |
| PS1CO2(2) | Fraction of C loss as CO ₂ during decomposition from soil metabolic pool | 0.55 | 0.4 | 0.8 |
| PS1S3(1) | Controls the amount of C loss as CO ₂ when soil structural decomposes to slow pool | 0.003 | 0.002 | 0.005 |
| PS1S3(2) | Intercept for clay effect on C transfer efficiency from active to passive pool during decomposition | 0.032 | 0.02 | 0.06 |
| PS2S3(1) | Slope for clay effect on C transfer efficiency during decomposition from active to passive pool | 0.003 | 0.002 | 0.005 |

Table 1 (continued)

| Model parameter | Description | Initial value | Lower bound | Upper bound |
|-----------------|---|---------------|-------------|-------------|
| PS2S3(2) | Intercept for clay effect on C transfer efficiency from slow to passive pool during decomposition | 0.009 | 0.006 | 0.013 |
| RCESTR(1) | Slope for clay effect on C transfer efficiency during decomposition from slow to passive pool | 100 | 50 | 300 |
| RIINT | C/N ratio for structural material, struc(1) and struc(2) | 0.5 | 0.2 | 0.7 |
| SNFXMX(1) | Root impact intercept used by rtimp; used for calculating the impact of root biomass on nutrient availability | 0.04 | 0.00001 | 1 |
| TEFF(1) | Symbiotic N fixation maximum for soybean g N/g C new growth | 15.4 | 5 | 30 |
| TEFF(2) | Temperature (degree C) at the inflection point for the temperature effect on decomposition | 0.27 | 0.15 | 0.5 |
| WEFF(1) | Slope of line at inflection point, for determining the temperature component of DEFAC | 30 | 25 | 35 |
| WEFF(2) | Moisture effect on decomposition | 9 | 6 | 15 |
| VARAT11(1_1) | Moisture effect on decomposition | 15 | 12 | 17 |
| VARAT11(2_1) | Maximum C/N ratio for material entering surface active pool | 6 | 4 | 6 |
| VARAT12(1_1) | Minimum C/N ratio for material entering surface active pool | 14 | 11 | 17 |
| VARAT12(2_1) | Maximum C/P ratio for material entering surface active pool | 3 | 2 | 4 |
| dmp | Minimum C/P ratio for material entering surface active pool | 0.003 | 0.001 | 0.01 |
| dmpflux | Damping factor for calculating soil temperature by layer | 8e-6 | 1e-6 | 1e-4 |
| N2Oadjust_fc | Dampens strong fluxes of water between soil layers | 0.025 | 0.001 | 1 |
| N2Oadjust_wp | Maximum proportion of nitrified N lost as N ₂ O at FC | 0.02 | 0.003 | 0.03 |
| FBM | Minimum proportion of nitrified N lost as N ₂ O at WP | 0.04 | 0.03 | 0.05 |
| FHP | Fraction of OC in biomass pool | 0.68 | 0.4 | 0.7 |

dimensions in the neighborhood. Therefore, it becomes more focused on local searches as the number of iterations approaches the specified maximum to keep the current gain in calibration results. Thus, DDS can rapidly converge to reasonable calibration solutions and avoid poor local optima. Several recent papers reported that the DDS algorithm works well in optimizing watershed models (Becker et al., 2019; Yen et al., 2015, 2016) and crop models (Wang et al., 2014; Choi et al., 2017; Shoaib et al., 2021).

The SCE-UA algorithm combines global exploration and local exploitation to search the parameter space efficiently. It also incorporates a shuffling mechanism, randomly exchanging members between different complexes. This shuffling helps exchange information among complexes and avoids premature convergence to suboptimal solutions. SEC-UA is known for its efficiency in navigating high-dimensional parameter spaces (Cooper et al., 1997; Ajami et al., 2004; Ayad et al., 2021).

DayCent-CUTE facilitates single and multiple site calibration and simulations (batch run) and automatically assembles user-selected model outputs (Fig. 1). The tool incorporates several Python libraries, such as NumPy, Matplotlib, and SciPy, for numerical computation, plotting, and statistical analyses. In addition, the GUI and process components are coded in *.ui and *.py files following an object-oriented programming style. To share the DayCent-CUTE program with other model users, the users need to have the same version of Python installed, along with all the libraries used. To avoid this tedious process, we use the cx-Freeze 6.3 to freeze the Python scripts into an executable. The executable and Python library files are then packaged into an installer file using the free installer program Inno Setup.⁴ Currently, the DayCent-CUTE program supports only Microsoft Windows 7 or higher.

A project must be created to run DayCent-CUTE for GSA or calibration. A project file (*.cproj) is made in the project folder, and DayCent input files used in the project are also copied into a subfolder called "TxtInOut." The input files in the "TxtInOut" are only used during SA or calibration runs but are not updated or deleted during the CUTE simulations. Once saved, the DayCent input files are copied to the "TxtWork," a working folder where the CUTE updates input parameters using sampled values and runs DayCent for assessment. In a sensitivity analysis project, the rank of parameter sensitivity resulting from a GSA is printed in the output files called "fastIndices.csv" or "sobolIndices.csv" depending on the method selected for GSA. The outputs include total sensitivity and first-order sensitivity of DayCent parameters to selected model outputs. Calibration results are summarized in several files including: sampled parameters and objective function values for all model iterations; model performance metrics during the iteration, such as coefficient of determination (R^2), model bias (Bais), the Nash-Sutcliffe efficiency (NSE), and root mean square error (RMSE).

2.4. Experimental study sites

A comprehensive literature review was undertaken to gather data for the calibration and evaluation of DayCent in simulating SOC dynamics using DayCent-CUTE. The review aimed to compile peer-reviewed and published studies pertaining to SOC. Experimental sites were selected based on the following criteria: (a) the studies must report sufficient information or any gaps in data should be reasonably inferable with minimal uncertainty to ensure effective site simulation; (b) SOC stocks should have been measured repeatedly over time (e.g., at least 2 twice in each experiment), allowing for the capture of SOC stock changes over time (e.g., over 3 to more than 100 years). This criterion ensures that the model accounts for practice effects on SOC and incorporates both short and long-term changes in soil biogeochemical processes; and (c) reported SOC measurements should correspond to a minimum depth of 30 cm, or the reported measurements should enable a reasonable estimation of SOC at the 30 cm depth through interpolation across the reported depths. Following the review and evaluation process, 30 sites (Fig. 2) were selected for calibrating and validating DayCent. The identified datasets comprise 215 combinations of management treatments with 581 measured SOC (excluding the initial/first-year measurements used to initialize soil C pools). Compiling the necessary model input files for each experimental site required gathering information from multiple relevant publications, including journal articles and book chapters. This approach was essential as long-term SOC measurements and the information needed for parameterizing DayCent were not always available in a single publication. The citations for all the publications used in compiling the model input files are provided in the citation columns of Table 2 for the respective site.

The dataset was randomly split into two sets for model calibration and independent evaluation, with a 60%–40% division across the 30 sites. The model calibration dataset comprised 18 experimental sites,

totaling 397 measurements (Table 2). The remaining 12 experimental sites were used for model evaluation and consisted of 220 measurements (Table 2). This resulted in an approximate split of 64% for calibration and 36% for evaluation. The experimental sites have well-documented management activities throughout the experiment, including crop rotation, cover crop usage, tillage practices, residue management, fertilizer application rates, irrigation, and organic amendments. These sites also provide reported edaphic characteristics such as soil texture and soil pH, which are necessary for conducting DayCent simulations. Meteorological data, encompassing daily minimum and maximum air temperature as well as precipitation, were extracted from the Parameter–Elevation Regressions on Independent Slopes Model (PRISM) database developed by the PRISM Climate Group.⁵ This data was obtained specifically for the experimental studies conducted in the United States (US). Weather data for US sites established before 1981 were extracted or gap-filled using DAYMET (Thornton et al., 2020) or local weather stations. These weather records were assembled with the experiments in the Agricultural Carbon Enhancement network (GRACENET) database.⁶ For sites located in the United Kingdom, the nearest weather station (as per Barré et al., 2010) was utilized. In the case of Canada,⁷ weather data was sourced from Environment and Climate Change Canada. Temperature and precipitation data for sites in Brazil were obtained from the SWAT global weather data.⁸ As for the Australian site, temperature data was acquired from SWAT, and precipitation data was obtained from the nearest weather station, specifically the Australian Government's Bureau of Meteorology.⁹

2.5. Global sensitivity analysis, model calibration and evaluation performance criteria

Although DayCent has a wide range of model parameters and DayCent-CUTE can facilitate over 50 parameter GSA and auto-calibration, for this particular study for SOC dynamics, we have selected 23 parameters (Table 3). Each of the 23 parameters was assumed to have an independent uniform prior distribution with lower and upper bounds listed in Table 1. These selected parameters directly or indirectly influence the dynamics of SOC by affecting the decay rate of soil carbon pools, carbon transfer efficiency, or crop productivity. The remaining parameters were left at their default values. For this study, the GSA was conducted using the FAST algorithm to identify the most influential parameters for SCE-UA calibration.

The model parameters were treated as population-level variables during the calibration process, and a multi-site calibration was performed for the 18 calibration sites. The SCE-UA algorithm was configured with a maximum number of iterations set to 5000, utilizing RMSE as the objective function for optimization. In addition to RMSE, which calculates the average squared differences between the predicted values and the observed values, where a lower RMSE indicates a higher level of accuracy in aligning the model's predictions with the actual data, other statistical analyses were employed to assess the model's performance in terms of quality and reliability compared to the observed values. The model bias was used to evaluate systematic under- or over-prediction and determine the magnitude of error. NSE was employed to assess how well the predicted values capture the overall trend of the observed data. R^2 was utilized to evaluate the model's accuracy in tracking the variation of observed values. Graphical comparisons were performed to assess the agreement between measured and modeled results. These

⁵ <https://prism.oregonstate.edu>.

⁶ <https://data.nal.usda.gov/dataset/gracenet-greenhouse-gas-reduction-through-agricultural-carbon-enhancement-network>.

⁷ Historical Data - Climate - Environment and Climate Change Canada (weather.gc.ca).

⁸ <https://swat.tamu.edu/data/cfsr>.

⁹ <http://www.bom.gov.au/climate/data/>.

⁴ <https://jrsoftware.org/>; last accessed on January 19, 2023.

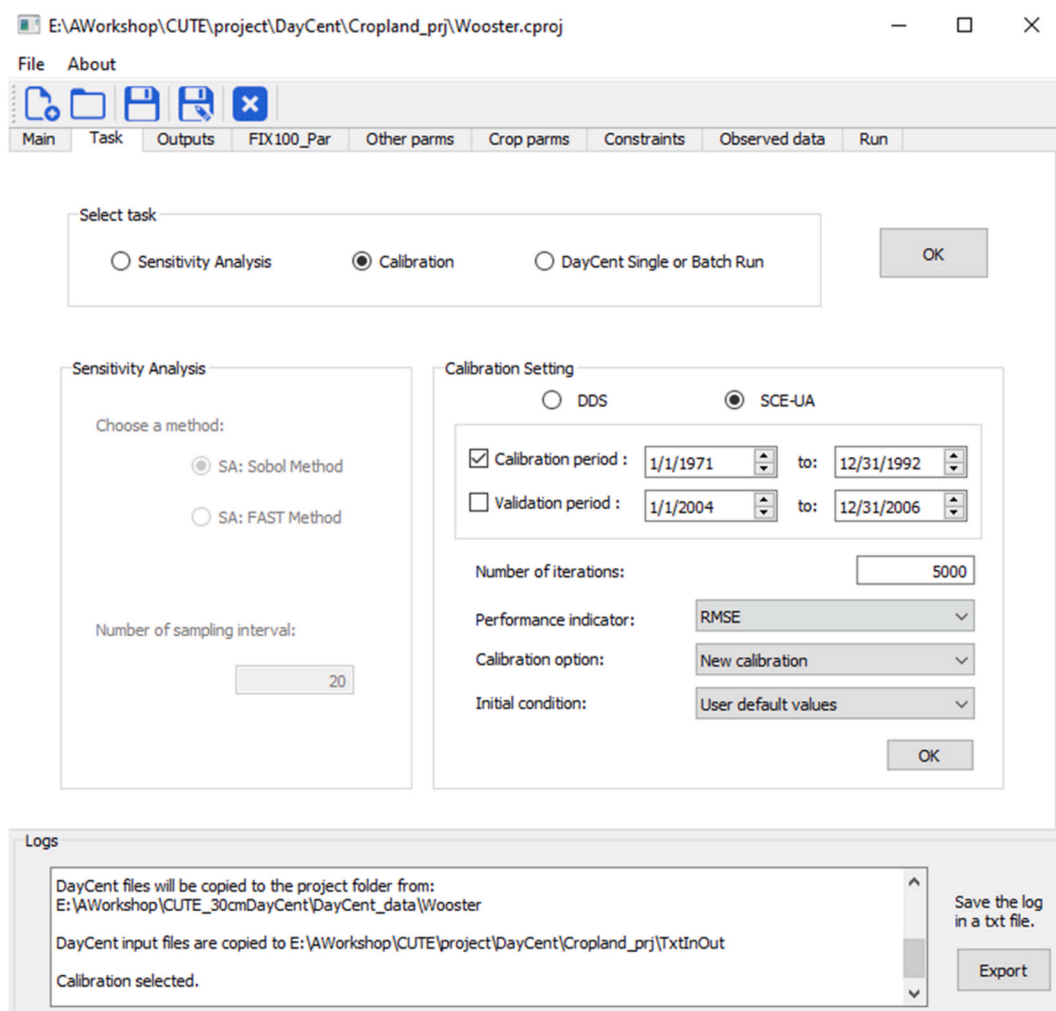


Fig. 1. DayCent-CUTE's GUI showing the Task tab.

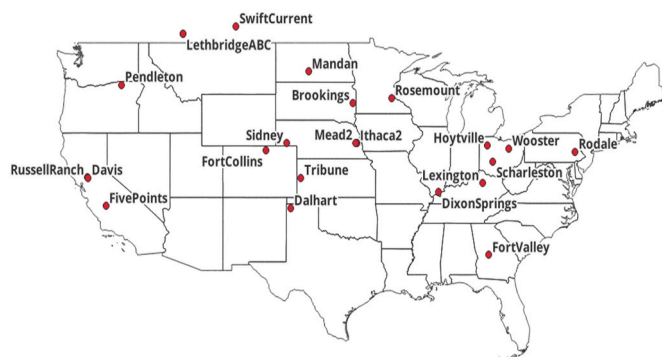


Fig. 2. Locations of the experimental sites used in this study (US and Canada sites only).

comparisons included scatterplots of model predictions versus measurements, histograms of residuals, and plots illustrating the 95% prediction intervals for SOC stocks and SOC stock differences between paired treatments. These additional statistical measures contribute to a comprehensive evaluation of the model's performance concerning the observed data.

3. Results and discussion

3.1. Parameter sensitivity on SOC estimation

The DayCent model was initialized with SOC stocks obtained from field measurements using Equations (1)–(3). Before conducting GSA, preliminary runs were carried out for all sites to verify the successful execution of the model with the provided inputs. The results demonstrated that the model initialization setup is realistic and appropriate. The realistic nature of the model initialization is supported by the overall model performance, as indicated by an R^2 value of 0.92 (Fig. 3), which represents the dataset in its initial state before model calibration. This R^2 value signifies a strong correlation between the model's predictions and the observed data, indicating the realistic model setup.

GSA was then performed across all 30 sites to obtain a better understanding of the DayCent model's behavior. DayCent saves the FAST S_{Ti} values of all 23 parameters used in GSA for each site. While the most influential parameters generally remain highly influential across study sites, the sensitivity indices are dynamic with S_{Ti} values vary among different sites (Fig. 4). This variation underscores the importance of conducting GSA for specific model applications, and ranking sensitivity indices is a means of identifying the crucial parameters responsible for the majority of model output variability (Wang et al., 2006). Utilizing the ranked mean S_{Ti} values, we selected the top 12 influential parameters for model calibration (Table 3). In two related studies conducted by Gurung et al. (2020) and Mathers et al. (2023), GSA was performed

Table 2

Experimental SOC study locations and treatments used for model calibration and evaluation. Treatment category abbreviations are CROPP: cropping practices (rotation, cover crops); NFERT: inorganic N fertilizer application (control, different levels of N rates); DISTU = soil disturbance and/or residue management (full till, no-till, reduced till); Omad: organic amendment (occurs in calibration dataset only); and n is the number of observations at the study location, excluding the initial measurements.

| Study: Calibration (18 sites; 397 obs) | Site location | Latitude | Longitude | Sand % | Silt % | Clay % | n obs | Duration (year) | Treatment | References |
|--|--------------------------------------|----------|-----------|--------|--------|--------|-------|-----------------|---------------------|---|
| Brookings | Brookings, SD, USA | 44.33 | -96.78 | 15 | 50 | 35 | 12 | 4 | CROPP, DISTR | Hammerbeck et al. (2012); Wegner et al. (2018) |
| Davis | Davis, CA, USA | 38.53 | -121.78 | 44 | 41 | 15 | 8 | 8 | CROPP, NFERT, Omad | Clark et al. (1998) |
| FivePoints | Five Points, CA, USA | 36.34 | -120.12 | 43 | 28 | 29 | 12 | 8 | CROPP, DISTR | Mitchell et al. (2015); Mitchell et al. (2017); Veenstra et al. (2006) |
| FortValley | Fort Valley, GA, USA | 32.53 | -83.89 | 65 | 25 | 10 | 36 | 3 | CROPP, DISTR, NFERT | Sainju et al. (2005) |
| Goias | Goias, Brazil | -17.84 | -50.6 | 28.8 | 21.7 | 49.5 | 4 | 9 | CROPP, DISTR | Ferreira et al. (2019) |
| Hoytville | Hoytville, OH, USA | 41.01 | -84.01 | 21 | 42 | 40 | 6 | 23 | CROPP, DISTR | Collins et al. (1999) |
| IthacaNE | Ithaca, NE, USA | 41.2 | -96.4 | 10 | 67 | 23 | 6 | 9 | DISTR | Jin and Varvel (2018) |
| Lethbridge | Lethbridge, AB | 49.7 | -112.83 | 15 | 85 | 34 | 8 | 25 | Omad | Hao et al. (2003) |
| LethbridgeABC | Lethbridge, AB | 49.7 | -112.83 | 38 | 31 | 31 | 18 | 79 | CROPP | Monreal and Janzen (1993) |
| Lexington | Lexington, KY, USA | 38.11 | -84.48 | 7 | 70 | 23 | 16 | 14 | DISTR, NFERT | Blevins et al. (1983); Ismail et al. (1994) |
| Mead 2 | Mead, NE, USA | 41.25 | -96.47 | 7 | 62 | 31 | 63 | 18 | CROPP, NFERT | Varvel (2006) |
| NarrabriFieldC1 | Narrabri, New South Wales, Australia | -30.2 | 149.6 | 26 | 21 | 53 | 21 | 19 | CROPP, DISTR | Senapati et al. (2014) |
| ORpegn | Pendleton, OR, USA | 45.72 | -118.63 | 12 | 70 | 18 | 67 | 79 | DISTR, NFERT, Omad | Bista et al. (2016); Ghimire et al. (2015); Rasmussen and Smiley (1997) |
| Rodale | Kutztown, PA, USA | 40.55 | -75.72 | 19.5 | 41.5 | 39 | 6 | 21 | NFERT | Elliott et al. (1994); Pimentel et al. (2005) |
| Saginaw | Saginaw, MI, USA | 43.38 | -84.11 | 9 | 44 | 47 | 12 | 19 | CROPP | Christenson (1997) |
| SwiftCurrent | Swift Current, SK | 50.28 | -107.8 | 37.5 | 26.5 | 36 | 24 | 43 | CROPP, NFERT | Campbell and Zentner (1997); Campbell et al. (2007) |
| Tribune | Tribune, KS, USA | 38.52 | -101.66 | 19 | 81 | 25.6 | 28 | 9 | CROPP, NFERT | Halvorson and Schlegel (2012) |
| Wooster | Wooster, OH, USA | 40.78 | -81.93 | 25 | 60 | 15 | 14 | 43 | CROPP, DISTR | Collins et al. (1999) and Dick et al. (1997) |
| Evaluation (12 sites, 220 obs) | | | | | | | | | | |
| Broadbalk | Rothamsted, England | 51.81 | -0.37 | 25 | 50 | 25 | 22 | 162 | NFERT | Rothamsted Research (2018) |
| Dalhart | Dalhart, TX, USA | 36.16 | -102.63 | 67 | 33 | 19 | 14 | 7 | CROPP, NFERT | Halvorson et al. (2009); Halvorson and Reule (2007) |
| DixonSprings | Dixon Springs, IL, USA | 37.43 | -88.66 | 23 | 77 | 19 | 27 | 20 | DISTR | Olson et al. (2010) |
| FortCollins | Fort Collins, CO, USA | 40.65 | -104.99 | 39 | 61 | 34 | 14 | 8 | DISTR | Halvorson et al. (2009) |
| Ithaca 2 | Ithaca (ithaca2), NE, USA | 41.2 | -96.4 | 10 | 58 | 32 | 3 | 13 | NFERT | Jin and Varvel (2018); Jin et al. (2015) |
| Mandan | Mandan, ND, USA | 46.77 | -100.95 | 28 | 51 | 21 | 36 | 13 | DISTR, NFERT | Halvorson et al. (2002) |
| NarrabriField6 | Narrabri, New South Wales, Australia | -30.2 | 149.6 | 26 | 21 | 53 | 25 | 10 | CROPP | Rochester (2011) |
| NarrabriFieldD1 | Narrabri, New South Wales, Australia | -30.2 | 149.6 | 26 | 21 | 53 | 28 | 10 | CROPP | Hulugalle et al. (2013) |
| Rosemount | Rosemount, MN, USA | 44.71 | -93.09 | 12.5 | 65 | 22.5 | 23 | 22 | DISTR, NFERT | Dolan et al. (2006) |
| RussellR | Winter, CA, USA | 38.54 | -121.87 | 18 | 59 | 23 | 19 | 19 | CROPP | Kong et al. (2005) |
| SCharleston | South Charleston, OH, USA | 39.8 | -83.5 | 15 | 65 | 20 | 6 | 32 | DISTR | Collins et al. (1999); Jarecki and Lal (2005) |
| Sidney | Sidney, NE, USA | 41.22 | -103.01 | 36 | 37.5 | 26.5 | 3 | 23 | DISTR | Elliott et al. (1994) |

using the Sobol method to evaluate the multi-site SOC dynamics in the DayCent model. Gurung et al. (2020) aggregated data from 19 long-term field experiments and employed 17 parameters for GSA. Out of the nine parameters highlighted as influential by Gurung et al. (2020), seven were also recognized as influential in our present study and six were recognized as influential by Mathers et al. (2023). The study by Mathers et al. (2023) involved data from 41 agricultural research sites and employed 28 parameters for GSA. Among the ten most influential parameters chosen for model calibration, seven were the same as those identified in our study. It is noteworthy that Gurung et al. (2020) ranked

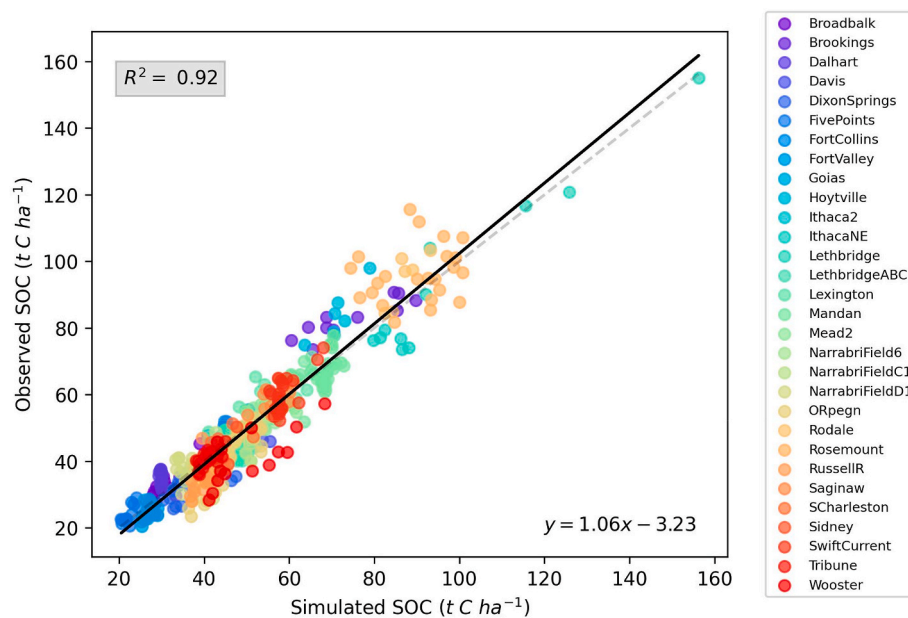
the maximum decomposition rate of the passive pool (DEC4) as the most influential parameter, whereas in our study and Mathers et al. (2023), it was ranked as the 12th influential parameter. Both the FAST and Sobol total sensitivity indices assess the combined influence of fractional parameter interactions on output variance across the entire parameter space. Varied parameter selections and experimental datasets in GSA may result in differing S_{Ti} values and rankings for these parameters.

Of the 12 identified parameters for model calibration, the first 5 are as follows: (1) optimum decomposition rate of soil slow organic matter (DEC5(2)), (2) fraction of the passive humus pool (FHP), (3) minimum

Table 3

Summary statistics of marginal posterior distributions of calibrated model parameters derived from the multi-site calibration process.

| Parameters | Posterior quantiles | | | | | Best fit |
|------------|---------------------|---------|---------|---------|---------|----------|
| | 2.50% | 25% | median | 75% | 97.50% | |
| ANEREF(2) | 2.9276 | 3.4071 | 3.6488 | 3.8633 | 4.2712 | 3.9794 |
| ANEREF(3) | 0.2616 | 0.4342 | 0.4726 | 0.5199 | 0.9386 | 0.4654 |
| DEC4 | 0.0017 | 0.0026 | 0.0029 | 0.0032 | 0.0039 | 0.0034 |
| DEC5(2) | 0.0527 | 0.0610 | 0.0657 | 0.0831 | 0.1987 | 0.0615 |
| FWLOSS(4) | 0.4824 | 1.4396 | 1.7470 | 1.7827 | 1.9387 | 1.7412 |
| P1CO2A(2) | 0.1303 | 0.1656 | 0.1729 | 0.1790 | 0.2103 | 0.1774 |
| P2CO2(2) | 0.3052 | 0.3273 | 0.3612 | 0.4561 | 0.7197 | 0.3303 |
| PMCO2(2) | 0.3977 | 0.4760 | 0.4857 | 0.4954 | 0.5973 | 0.4821 |
| TEFF(1) | 8.8240 | 13.3031 | 14.1964 | 17.1022 | 23.5947 | 14.3776 |
| TEFF(2) | 0.1572 | 0.2680 | 0.3602 | 0.4530 | 0.4939 | 0.4703 |
| WEFF(2) | 7.7426 | 10.8406 | 12.4803 | 13.8124 | 14.7638 | 13.9155 |
| FHP | 0.4737 | 0.5427 | 0.5611 | 0.6005 | 0.7418 | 0.5425 |

**Fig. 3.** Preliminary simulation using DayCent default parameter values and initial SOC measurements from 30 study sites for initialization of soil carbon pools.

value of the impact of anaerobic soil conditions on decomposition (ANEREF(3)), which functions as a multiplier for the maximum decomposition rate, (4) the effect of temperature on decomposition (TEFF(1)), and (5) a scaling factor related to soil water (FWLOSS(4)) that influences potential evapotranspiration. Additionally, the moisture effect on decomposition (WEFF(2)) also has a substantial impact on the dynamics of soil carbon (Fig. 4).

3.2. Posterior model parameters

The SCE-UA calibration for the 18 experimental sites reached convergence after 2275 iterations (Fig. 5). This assertion is corroborated by the presence of a low normalized geometric range, which signals the optimization process is concentrating on a narrower parameter value range. Furthermore, the improvement rate of the RMSE over the last three iterations was a mere 0.08%. As a result, the calibrated parameters now exhibit marginal posteriors with narrower ranges and higher densities (Fig. 6), in contrast to the initially assumed uniform priors. This indicates that the measurement dataset provided informative constraints for the SCE-UA calibration process. Notably, influential parameters such as DEC5(2), TEFF(1), FWLOSS(4), PMCO2(2), P1CO2A(2), and FHP demonstrate a significant reduction in uncertainty compared to their uniform priors, which span the parameter space. The 95% posterior intervals of the optimum decay rates for the slow and

passive pools are reported to range between 0.0527 and 0.1987 (DEC5(2)) and 0.0017 to 0.0039 (DEC4), respectively (Table 3). These intervals imply turnover times ranging from 5 to 19 years for the slow pool and 260–580 years for the passive pool. These findings align with the results reported by Gurung et al. (2020), where they observed turnover times between 6 and 14 years for the slow pool and 200–500 years for the passive pool based on the calibration of 8 long-term experimental sites (a total of 19 sites were reported in their study). The parameter TEFF(1), associated with the temperature effect on decomposition, varies between 9 and 24 °C, peaking around 14 °C (Table 3 and Fig. 6). This suggests that decomposition is most sensitive to temperature changes within this particular temperature range.

3.3. Posterior model prediction and performance evaluation

The SCE-UA calibration resulted in posterior parameter distributions that demonstrated significantly decreased model bias compared to the prior parameter distribution results (Fig. 7). For instance, the median values of model bias were 0.34 and 2.35 t C ha⁻¹ from posterior and prior calibration, respectively. The calibration yielded a reduced RMSE with median values of 4.56 t C ha⁻¹, in contrast to 7.97 t C ha⁻¹ in the prior distribution. Furthermore, it achieved higher NSE scores, with an increase from 0.82 to 0.92, and enhanced R² values, improving from 0.88 to 0.94. As anticipated, the model's performance statistics are

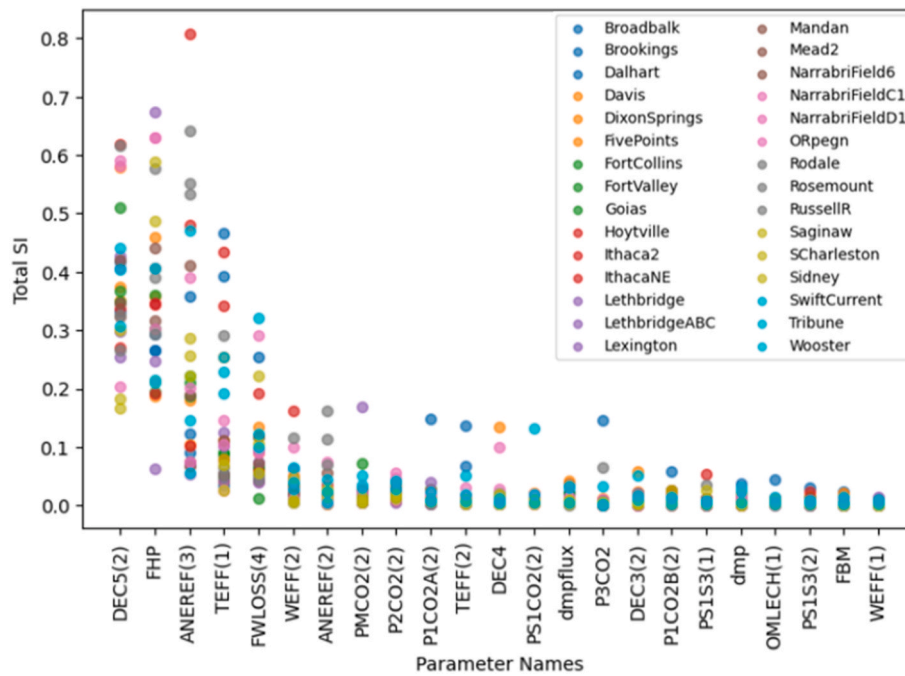


Fig. 4. Ranked DayCent parameters based on the means of FAST total sensitivity indices across the 30 field experiments used in this study for SOC simulation.

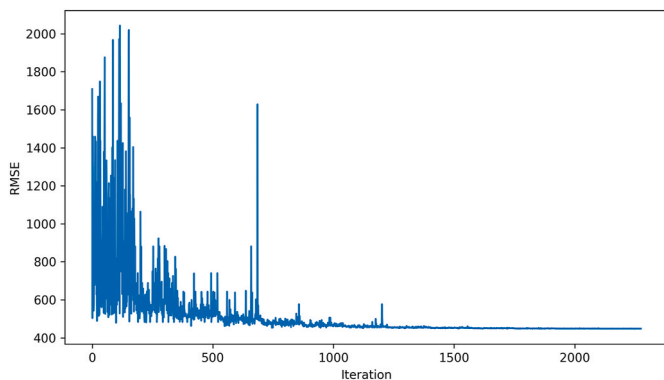


Fig. 5. Convergency of the Shuffled Complex Evolution algorithm for DayCent parameter calibration across 18 field experiments in the multi-site calibration process.

better for the calibration dataset than for the evaluation dataset, reflecting the model’s parameterization tailored to these specific locations. Nonetheless, it’s worth highlighting that the model’s performance metrics for posterior evaluation surpass those for prior calibration, as illustrated by the probability density distribution in Fig. 7, where the model bias is $-0.73 \text{ t C ha}^{-1}$ (compared to 2.35), RMSE is 6.84 t C ha^{-1} (compared to 7.97), and NSE is 0.87 (compared to 0.82).

The simulations based on the posterior parameter distribution displayed a distribution of predicted median values and measured SOC values that clustered around the 1:1 line (Fig. 8). The calibration and evaluation datasets demonstrated a positive association between the measured and modeled SOC stocks. This indicates a close agreement between the measured and modeled values. Notably, the calibrated model realistically predicted both low and high SOC values for both datasets, with the average value of simulated SOC stocks closely matching the mean of measured SOC stocks (Fig. 8). The relationship between the measured and modeled SOC stocks was stronger in the calibration dataset.

In the calibration dataset, the coefficient of variation (CV), a statistical measure that normalizes the dispersion of a probability

distribution, for measured SOC stocks stands at 36%, with a corresponding mean value of 49.1 t C ha^{-1} . Conversely, the CV for simulated SOC stocks across the 18 calibration sites is marginally lower, registering at 34%. In the evaluation dataset, the CV for measured SOC stocks is 42%, with a mean of 48.9 t C ha^{-1} , while the CV for simulated SOC stocks is also slightly lower at 38%. This suggests that, in both the calibration and evaluation datasets, the measured SOC data exhibits a slightly higher degree of relative variability compared to the simulated SOC data, although the difference is relatively small. The disparity in CV values between measured SOC stocks and DayCent model simulations can be attributed to various factors, including: (1) Measurement error: The data collected for SOC stocks can introduce higher variability in the measured values due to several sources of error, such as sampling variability, laboratory analysis, and instrument precision. These measurement errors can consequently inflate the observed CV for measured SOC stocks; (2) Spatial and temporal variability: SOC stocks in the real world often exhibit substantial spatial and temporal variations driven by factors such as soil type, land management practices, and climate fluctuations. These natural variations may result in higher CV values in measured data. In contrast, DayCent, functioning as a point simulation model, primarily captures the dominant characteristics of each field experimental site; (3) Model assumptions: models like DayCent simplify and make deterministic assumptions about how SOC behaves in the environment. This can lead to more consistent and less variable model outputs.

While we treated the model parameters as population-level variables during the calibration process, resulting in posterior distributions of model parameters suitable for application to the entire range of soils and climatic conditions represented by these experiments, as well as for new testing sites within the geographical domain, DayCent-CUTE users also have the option to select a single optimized parameter set tailored to their specific research needs. In this study, Fig. 9 presents the model performance for the best fit parameter set (Table 3). The model effectively explains approximately 94% and 93% (with R^2 values of 0.94 and 0.93) of the variance in the observed SOC stocks for the calibration and independent evaluation datasets, respectively. Given the range of measured SOC stocks (from 20.4 to $155.1 \text{ t C ha}^{-1}$), the RMSE value of 4.49 t C ha^{-1} indicates a reasonable prediction error for the calibration dataset. For the evaluation dataset, where the measured SOC stocks

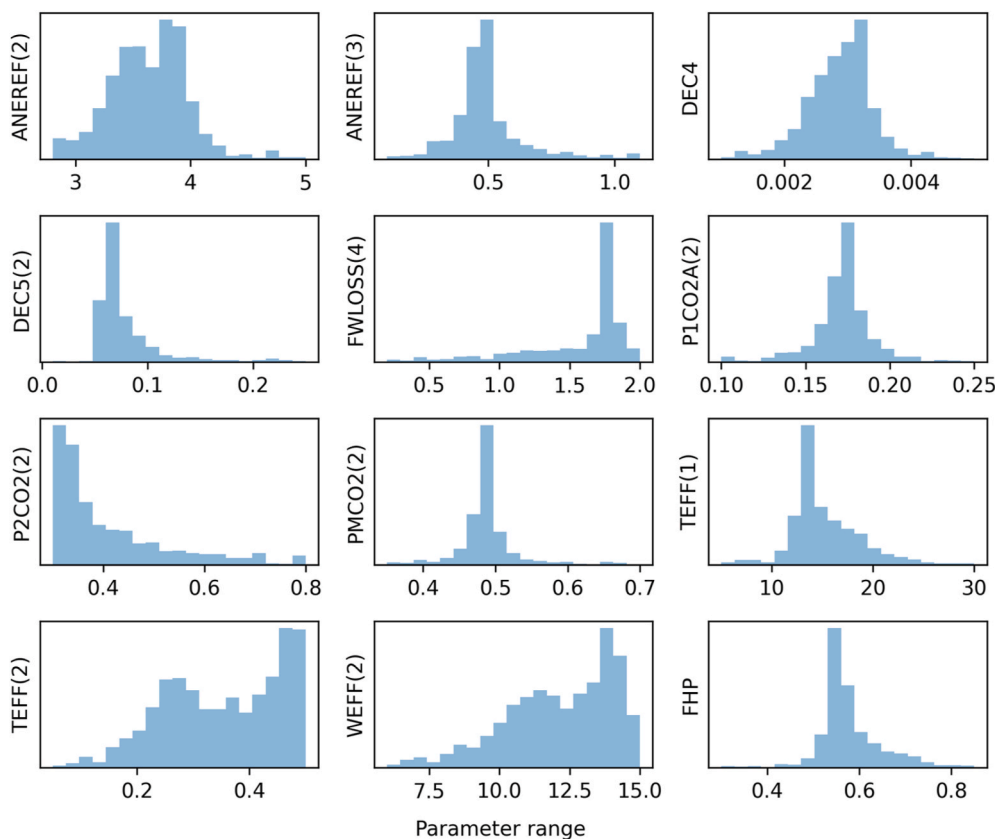


Fig. 6. Marginal posterior density of DayCent parameters from multi-site calibration.

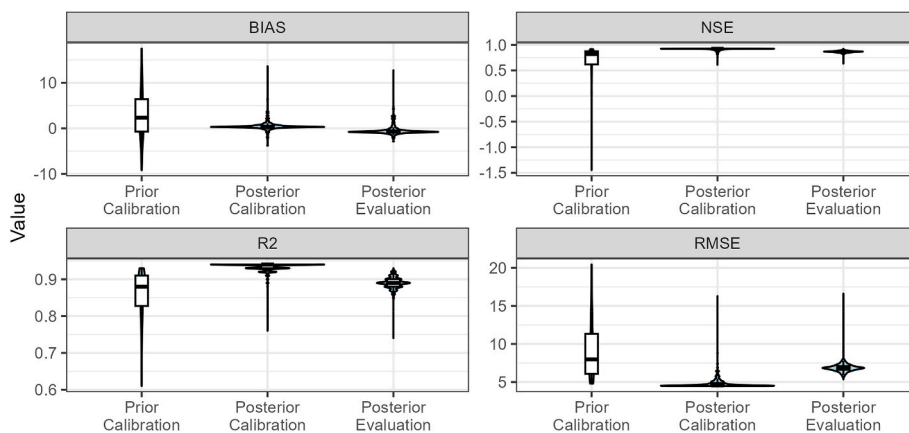


Fig. 7. Violin plots showing the distributions of model performance metrics for the prior and posterior modeling comparisons between simulated and measured SOC stocks in the calibration and evaluation dataset. The bias and RMSE units are in $t C ha^{-1}$.

range from 23.8 to 115.6 $t C ha^{-1}$, the RMSE value of 5.35 $t C ha^{-1}$ suggests a slightly higher level of prediction error. The NSE values of 0.93 and 0.92 were obtained for the calibration and evaluation datasets, respectively, indicating that the calibrated DayCent model effectively captures the SOC dynamics across multiple sites in a realistic manner. This also demonstrated that using directly measured SOC and tuning model parameters for the initialization of soil C pools overcome the difficulties present in the classical method of model spin-up initialization, especially for those sites where the previous land use history is unknown. The optimization results at the 30 experimental study sites show that the DayCent model realistically simulated the effects of various management strategies on SOC stocks without an equilibrium iteration.

As previously discussed, the evaluation dataset exhibits a greater variability in measured SOC stocks compared to the calibration dataset, with CV values of 42% and 36%, respectively. While the posterior model predictions successfully capture the variability in the measured SOC stocks within the evaluation dataset, we observed significant under-predictions for the majority of SOC comparison points at the Rosemount site and over-predictions for most SOC comparison points at the Broadbalk site in the evaluation dataset (see Fig. 8b). However, the parameter set that provides the best fit presents a much more balanced distribution of under- and over-predictions for these sites as shown in Fig. 9b.

The improved performance exhibited by this parameter set suggests the possibility of selecting a parameter combination suitable for reducing uncertainty within a specific sub-population when

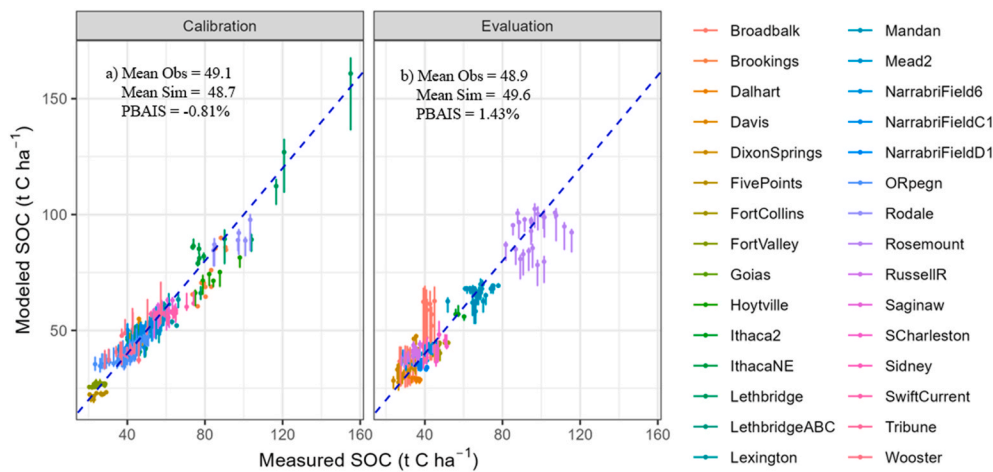


Fig. 8. Comparison of SOC stocks between measured and the posterior medians (depicted as dots) along with the 95% central posterior prediction interval for the calibration and evaluation datasets. The dashed diagonal line represents the 1:1 relationship.

implementing the DayCent model. However, it's important to acknowledge that this choice may also limit the model's applicability to various sites or regions, contingent upon the availability of parameterization data. When faced with varying environmental conditions and diverse management practices across different geographical locations, the posterior distribution of model parameters obtained from this study empowers the DayCent model to extend its application to simulate SOC dynamics beyond the scope of the experimental sites examined in this study. The resulting 95% central posterior prediction interval can be used for quantifying the uncertainty of model predictions. Choosing one optimized deterministic model or a generalized model with joint posterior distribution for model parameters depends on the precise objectives and constraints of the analysis or application. In certain instances, a hybrid approach may be advantageous, where an initial application of a generalized model is followed by site-specific refinements. These refinements involve incorporating site-specific data and adjustments into the modeling process when ample site-specific information is at hand. Such integration serves to boost accuracy and can be achieved through the use of DayCent-CUTE.

While DayCent was calibrated and validated for SOC stocks in the top 0–30 cm of agricultural soils, the SOC stock change rate (ΔSOC in $\text{t C ha}^{-1} \text{ yr}^{-1}$) in response to management practice changes were also evaluated (Fig. 10). This represents a more rigorous validation, as the per year SOC stock changes involves comparing pairwise treatment differences over the years elapsed. Since the model was calibrated with unified parameter sets for all treatments. These generalized models had no specific calibration for individual treatments. Consequently, to account for treatment differences effectively, it is crucial for the model to accurately capture the interactions between management practices and carbon sequestration processes within its underlying biogeochemical representations.

When comparing various pairwise combinations of cropping practices (continuous cropping, rotations, cover cropping), different inorganic N fertilization rates (ranging from 0 to 224 kg N ha^{-1}), and different levels of soil disturbance (e.g., no-till, reduced till, chisel tillage, conventional tillage), we observed that the measured ΔSOC change rates and standard deviations (SD) were generally higher than the simulated ΔSOC rates, even for the calibration datasets (Fig. 10). This indicates that the model leans towards conservatism, consistently underpredicting SOC stock changes, aligning with the observations made by Mathers et al. (2023). In their study, Mathers et al. noted that DayCent demonstrates a conservative behavior by under-predicting SOC changes when SOC increases compared to counterfactual baselines across 14 pairs of crop functional group and practice category combinations within the dataset from 41 sites. In the context of carbon

crediting markets, the most critical metric is quantifying the change in response to management practices. While underestimation is preferable to avoid overcrediting in carbon-crediting programs, the consistent underestimation of SOC change rates raises several important implications and considerations.

Firstly, the model may not adequately capture the interactions between management practices and carbon cycling processes, including decomposition rates (with decomposition parameters derived from the multi-site, multi-treatment SOC dataset used for model parameterization), vegetation growth, or carbon inputs. This lack of accuracy may not effectively capture real-world conditions. However, as science advances and our understanding of plant litter decomposition, SOM formation, and microbial dynamics improves, coupled with the availability of more informative and representative datasets for testing our understanding, the process-based representation of SOM dynamics can be enhanced. This, in turn, has the potential to reduce model structure and parameter uncertainty.

Additionally, it's worth noting that measured SOC changes typically exhibit a higher degree of variability or noise, as evidenced by the broader ranges of measured SOC change rate in both the calibration and evaluation datasets (Fig. 10), due to several significant factors: First, natural variability plays a key role, as SOC levels can naturally fluctuate in agricultural fields, influenced by variations in plant productivity and microbial activity. Consequently, SOC measurements taken at different time points may inherently display fluctuations, even in the absence of intentional management changes. Second, measurement errors introduce another layer of complexity, as different measurement methods, laboratories, and instruments can yield slightly divergent results of the SOC data. Additionally, soil sampling location can introduce variability over the measurement period, contributing to the observed noise in SOC change data. Third, temporal lags in SOC changes' responses to alterations in management practices are common. This delayed response can result in observed variations in SOC data. Often, SOC measurements are taken at one time during the year, whereas annual average SOC modeling outputs are typically used to represent the SOC stock for the entire year, creating a temporal discrepancy that makes it more challenging to discern immediate cause-and-effect relationships. Finally, spatial variability within a field or ecosystem, driven by factors like topography, soil texture, and historical land management practices, can contribute to variations in measured SOC changes. Smaller sample sizes may also exacerbate the noise within the data. Consequently, when comparing pairwise treatment model outputs to measurements of SOC change rates, it often entails more substantial uncertainties than when comparing SOC stocks. While not explicitly evaluated in this study, it is essential to acknowledge that uncertainty inherent in measured data can

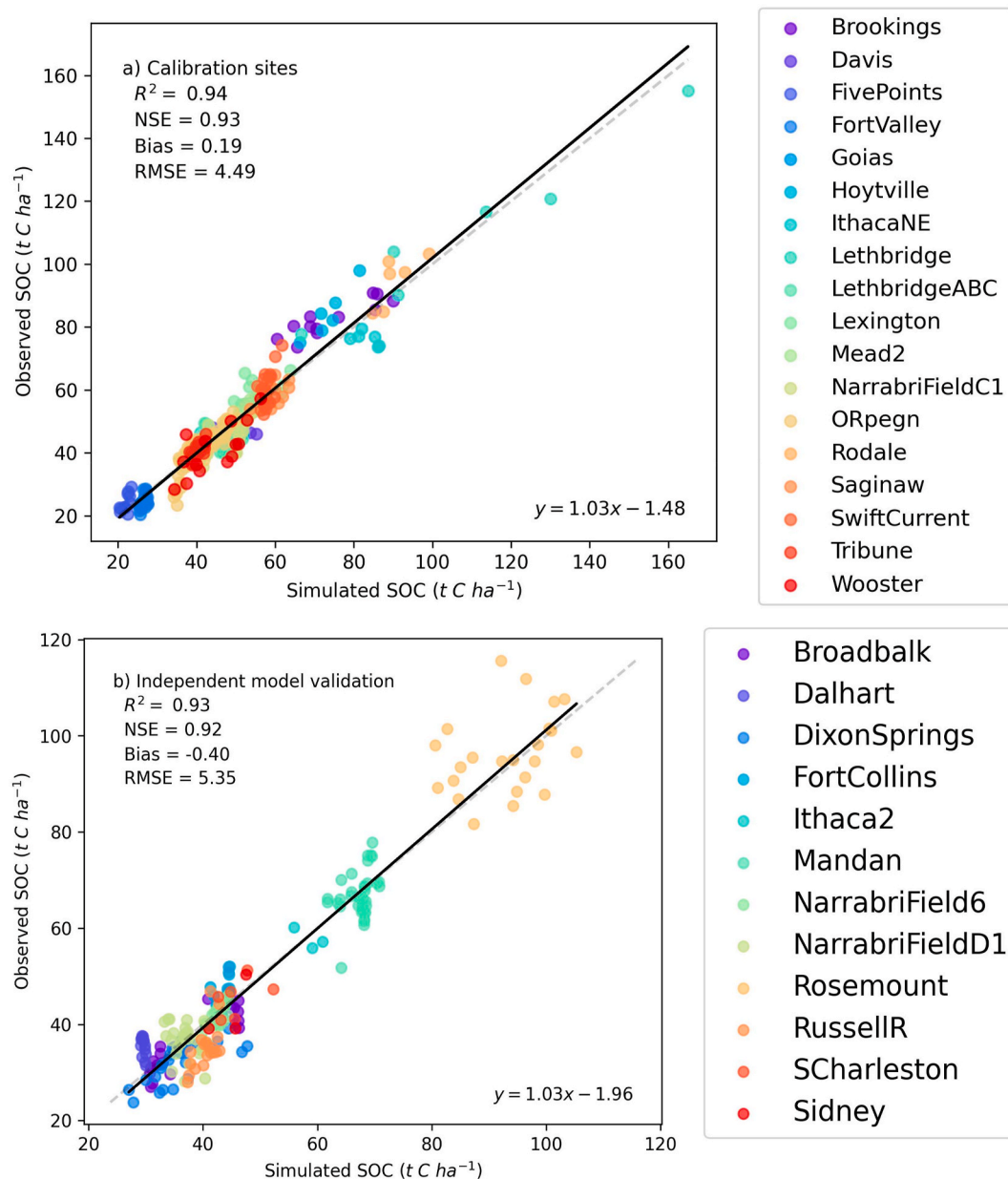


Fig. 9. Comparison of simulated and observed SOC stocks using the optimized parameter set for a) the calibration dataset and b) the independent evaluation dataset.

impact model parameterization and the reliability of calibrated models (Harmel et al., 2006).

4. Conclusion and future work

In this study, we developed DayCent-CUTE, a Python-based GUI program, to facilitate parameter sensitivity analysis, calibration, and uncertainty analysis of the DayCent model. The GSA and SCE-UA parameterization methods were employed as objective approaches for evaluating the DayCent model's performance. The current version, DayCent-Cute ver. 1.0, can be used to evaluate over 50 DayCent parameters and identify influential parameters for subsequent calibration. By examining 30 peer-reviewed experimental studies, we demonstrated the successful application of the GSA-FAST method in identifying significant parameters that influence SOC prediction. The combined utilization of GSA and SCE-UA methods effectively reduces uncertainty in model predictions of SOC, as indicated by posterior predictions for SOC estimates.

While population-based parameters were derived from a multi-site, multi-treatment SOC stock dataset for model parameterization, representing SOC stock change rates is inherently more challenging than depicting SOC stocks. In the context of carbon crediting markets, the quantification of SOC stock differences resulting from adopted practices is the pivotal metric of concern. This underscores the need for an enhanced scientific representation of the intricate interactions between management practices and SOM dynamics within the process-based model structure, accompanied by a more rigorous dataset encompassing both model inputs and measured SOC stocks. The DayCent-CUTE tool enables continuous model updates to incorporate new datasets and improvements in model structure as they emerge from future research.

To further enhance the performance of DayCent-CUTE on high-dimensional optimization problems, we are currently developing and exploring the implementation of a self-adaptive Differential Evolution learning strategy within a population-based evolutionary framework known as Differential Evolution Adaptive Metropolis (DREAM) (Vrugt

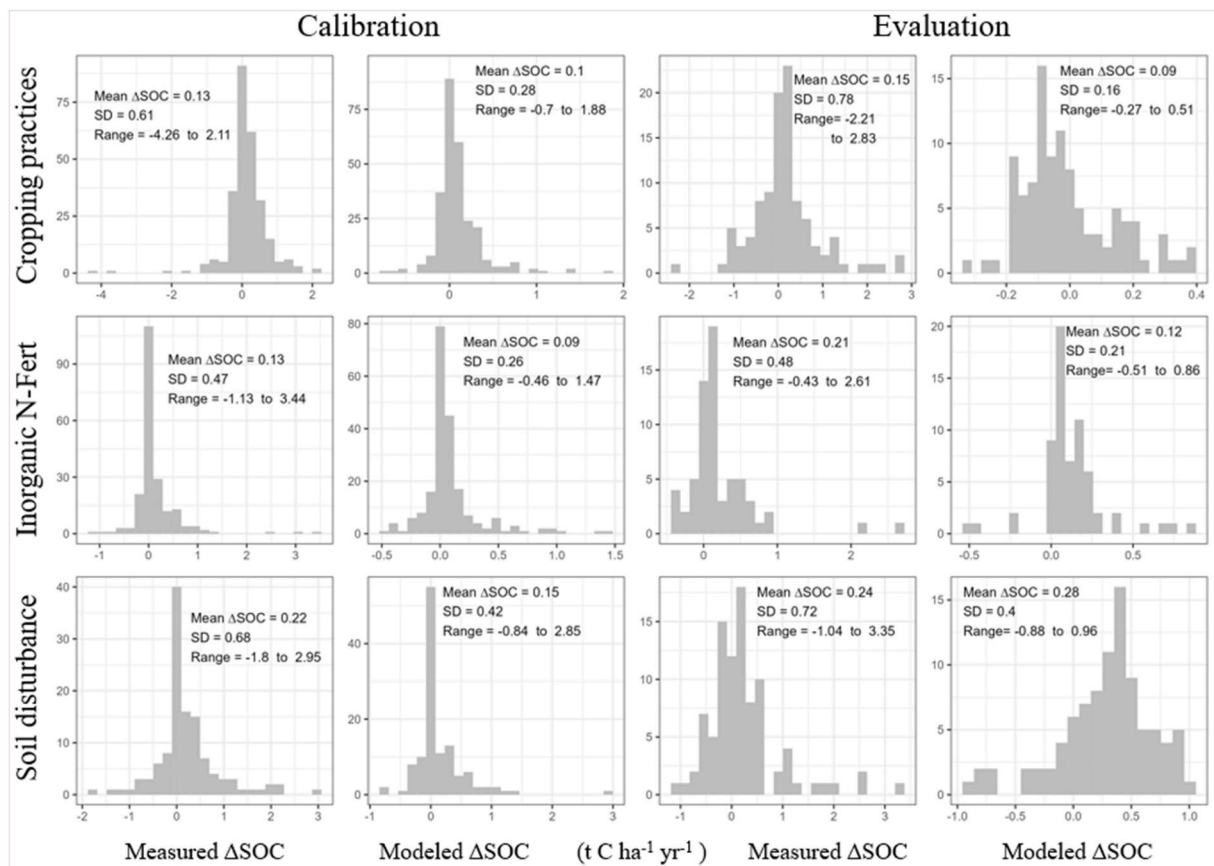


Fig. 10. Histogram depicting the measured and modeled SOC stock change rates for different cropping practices, including rotations or cover cropping (top), different inorganic N fertilization rates (middle), and various levels of soil disturbance (bottom).

et al., 2008, 2009). Integrating different algorithms into DayCent-CUTE will facilitate parallel processing through a multi-chain method. Overall, the DayCent-CUTE program is expected to serve as a user-friendly tool for parameter calibration and uncertainty analysis, enabling the application of the DayCent model to assess SOC dynamics under various management practices. This will provide valuable scientific information to support the development of climate-smart agriculture practices.

Declaration

Dr. Xuesong Zhang was supported in part by the U.S. Department of Agriculture, Agricultural Research Service. USDA is an equal opportunity provider and employer. Mention of trade names or commercial products in this publication is solely to provide specific information and does not imply recommendation or endorsement by the U.S. Department of Agriculture.

Declaration of competing interest

The authors declare that they have no known competing financial interests or personal relationships that could have appeared to influence the work reported in this paper.

Data availability

Data will be made available on request.

Acknowledgments

We express our gratitude to Dr. Melannie Hartman of Colorado State University (CSU) for her generous provision of the DayCent source code

and for engaging in valuable discussions. While we utilized an updated version of DayCent in our tool, Dr. Hartman's workshop training dataset was instrumental in helping us kickstart our project. We are also grateful to Dr. S.J. Del Grosso of USDA-ARS for providing us with essential database sources. Furthermore, our heartfelt appreciation goes to Dr. Ram Gurung of CSU and Dr. John Field of the Oak Ridge National Laboratory (ORNL) for their invaluable feedback during the revision process. We also extend our thanks to anonymous reviewers for their constructive suggestions, which greatly contributed to enhancing the quality of this work. This work was supported and funded by Agoro Carbon Alliance US., Inc.

References

- Ajami, N.K., Gupta, H., Wagener, T., Sorooshian, S., 2004. Calibration of a semi-distributed hydrologic model for streamflow estimation along a river system. *J. Hydrology* 298 (1–4), 112–135. <https://doi.org/10.1016/j.jhydrol.2004.03.033>.
- Allison, F.E., 1973. U.S. Department of Agriculture, Washington, D.C., U.S.A.. In: Allison, F.E. (Ed.), *Soil Organic Matter and its Role in Crop Production*, vol. 3. Elsevier Scientific Publ, Amsterdam, pp. 3–637, 1973.
- Ayad, A., Khalifa, A., Fawy, M.E., Moawad, A., 2021. An integrated approach for non-revenue water reduction in water distribution networks based on field activities, optimisation, and GIS applications. *Ain Shams Eng. J.* 12 (4), 3509–3520. <https://doi.org/10.1016/j.asej.2021.04.007>.
- Barré, P., Eglin, T., Christensen, B.T., Ciais, P., Houot, S., Kätterer, T., van Oort, F., Peylin, P., Poulton, P.R., Romanenkov, V., 2010. Quantifying and isolating stable soil organic carbon using long-term bare fallow experiments. *In. Biogeosciences* 7 (11), 3839–3850. <https://doi.org/10.5194/bg-7-3839-2010>.
- Becker, R., Koppa, A., Schulz, S., Usman, M., Beek, T.A.D., Schuth, C., 2019. Spatially distributed model calibration of a highly managed hydrological system using remote sensing-derived ET data. *J. Hydrol.* 577.
- Bista, P., Machado, S., Ghimire, R., Del Grosso, S.J., Reyes-Fox, M., 2016. Simulating soil organic carbon in a wheat–fallow system using the DAYCENT model. *Agron. J.* 108, 2554–2565.

- Blevins, R.L., Thomas, G.W., Smith, M.S., Frye, W.W., Cornelius, P.L., 1983. Changes in soil properties after 10 years continuous non-tilled and conventionally tilled corn. *Soil Tillage Res.* 3, 135–146.
- Byrne, K.A., Kiely, G., 2008. Evaluation of Models (PaSim, RothC, CENTURY and DNDC) or Simulation of Grassland Carbon Cycling at Plot, Field and Regional Scale. 2005-FS-32-M1. STRIVE Report. Prepared for the Environmental Protection Agency.
- Campbell, C.A., Zentner, R.P., 1997. Crop production and soil organic matter in long-term crop rotations in the semi-arid northern Great Plains of Canada. In: Paul, E.A., Paustian, K., Elliot, E.T., Cole, C.V. (Eds.), *Soil Organic Matter in Temperate Agroecosystems - Long Term Experiments in North America*. CRC Press, pp. 317–334.
- Campbell, C.A., VandenBygaart, A.J., Zentner, R.P., McConkey, B.G., Smith, W., Lemke, R., Grant, B., Jefferson, P.G., 2007. Quantifying carbon sequestration in a minimum tillage crop rotation study in semiarid southwestern Saskatchewan. *Can. J. Soil Sci.* 235–250.
- Carvalhais, N., Reichstein, M., Seixas, J., Collatz, G.J., Pereira, J.S., Berbigier, P., Carrara, A., Granier, A., Montagnani, L., Papale, D., Rambal, S., Sanz, M.J., Valentini, R., 2008. Implications of the carbon cycle steady state assumption for biogeochemical modeling performance and inverse parameter retrieval. *Global Biogeochem. Cycles* 22.
- Choi, S.K., Jeong, J., Kim, M.K., 2017. Simulating the effects of agricultural management on water quality dynamics in rice paddies for sustainable rice production-model development and validation. *Water* 9 (11).
- Christensen, B.T., 1996. Matching measurable soil organic matter fractions with conceptual pools in simulation models of carbon turnover: revision of model structure. *Evaluation of soil organic matter models* 143–159.
- Christenson, D.R., 1997. Soil organic matter in sugar beet and dry bean cropping systems in Michigan. In: Paul, E.A., Paustian, K., Elliot, E.T., Cole, C.V. (Eds.), *Soil Organic Matter in Temperate Agroecosystems - Long-Term Experiments in North America*. CRC Press, pp. 151–159.
- Clark, M.S., Horwath, W.R., Shennan, C., Scow, K.M., 1998. Changes in soil chemical properties resulting from organic and low-input farming practices. *Agron. J.* 90, 662–671.
- Climate Action Reserve, 2022. *Soil-Enrichment-Protocol-V.1.1-final.pdf*. climateactionreserve.org. (Accessed 2 January 2023).
- Collins, H.P., Blevins, R.L., Bundy, L.G., Christenson, D.R., Dick, W.A., Muggins, D.R., Paul, E.A., 1999. Soil carbon dynamics in corn-based agroecosystems: results from carbon-13 natural abundance. *Soil Sci. Soc. Am. J.* 63 (3), 584–591. <https://doi.org/10.2136/sssaj1999.03615995006300030022x>. Issn: 03615995.
- Cooper, V.A., Nguyen, V.T.V., Nicell, J.A., 1997. Evaluation of global optimization methods for conceptual rainfall-runoff model calibration. *Water Sci. Technol.* 36 (5), 53–60. <https://doi.org/10.2166/wst.1997.0163>.
- Dangal, S.R., Schwalm, C., Cavigelli, M.A., Gollany, H.T., Jin, V.L., Sanderman, J., 2022. Improving soil carbon estimates by linking conceptual pools against measurable carbon fractions in the DAYCENT Model Version 4.5. *J. Adv. Model. Earth Syst.* 14 (5), e2021MS002622.
- Del Grosso, Parton, W.J., Keough, C.A., Reyes-Fox, M., 2011. Features of the DayCent modeling package and additional procedures for parameterization, calibration, validation, and applications. In: Ahuja, L., Ma, L. (Eds.), *Methods of Introducing System Models into Agricultural Research, Advances in Agricultural Systems Modeling Series*, vol. 2.
- Del Grosso, S.J., Parton, W.J., Mosier, A.R., Hartman, M.D., Brenner, J., Ojima, D.S., Schimel, D.S., 2001. Simulated interaction of carbon dynamics and nitrogen trace gas fluxes using the DAYCENT model. In: Schaffer, M., Ma, L., Hansen, S. (Eds.), *Modeling Carbon and Nitrogen Dynamics for Soil Management*. CRC Press, Boca Raton, Florida, p. 303e332.
- Del Grosso, S.J., Mosier, A.R., Parton, W.J., Ojima, D.S., 2005. DAYCENT model analysis of past and contemporary soil N₂O and net greenhouse gas flux for major crops in the USA. In: *Soil and Tillage Research*.
- Del Grosso, S.J., Ogle, S.M., Parton, W.J., Breidt, F.J., 2010. Estimating uncertainty in N₂O emissions from U.S. cropland soils. *Global Biogeochem. Cycles* 24, GB1009. <https://doi.org/10.1029/2009GB003544>.
- Del Grosso, S.J., Parton, W.J., Mosier, A.R., Walsh, M.K., Ojima, D.S., Thornton, P.E., 2006. DAYCENT National-scale simulations of nitrous oxide emissions from cropped soils in the United States. *J. Environ. Qual.* 35, 1451–1460. <https://doi.org/10.2134/jeq2005.0160>.
- Dick, W.A., Edwards, W.M., McCoy, E.L., 1997. Continuous application of no-tillage to Ohio soils: changes in crop yields and organic matter-related soil properties. In: Paul, E.A., Paustian, K., Elliot, E.T., Cole, C.V. (Eds.), *Soil Organic Matter in Temperate Agroecosystems. Long-Term Experiments in North America*. CRC Press, pp. 171–182.
- Dolan, M.S., Clapp, C.E., Allmaras, R.R., Baker, J.M., Molina, J.A.E., 2006. Soil organic carbon and nitrogen in a Minnesota soil as related to tillage, residue and nitrogen management. *Soil Tillage Res.* 89, 221–231.
- Duan, Q.Y., Gupta, V.K., Soroshian, S., 1993. Shuffled complex evolution approach for effective and efficient global minimization. *J. Optimiz. Theory Appl.* 76, 501–521. <https://doi.org/10.1007/BF00939380>.
- Elliott, E.T., Burke, I.C., Monz, C.A., Frey, S.D., Paustian, K.H., Collins, H.P., Paul, E.A., Cole, C.V., Blevins, R.L., Frye, W.W., Lyon, D.J., Halvorson, A.D., Huggins, D.R., Turco, R.F., Hickman, M.V., 1994. Terrestrial carbon pools: preliminary data from the corn belt and great plains regions. In: Doran, W., Coleman, D.C., Bezdicek, D.F., Stewart, B.A. (Eds.), *SSSA Special Publications*. Soil Science Society of America, pp. 179–191.
- Feng, Q., Chaubey, I., Her, Y.G., Cibir, R., Engel, B., Volencic, J., Wang, X., 2015. Hydrologic and water quality impacts and biomass production potential on marginal land. *Environ. Model. Software* 72, 230–238.
- Ferreira, A.C. de B., Borin, A.L.D.C., Lamas, F.M., Bogiani, J.C., da Silva, M.A.S., Filho, J. L. da S., Staut, L.A., 2019. Soil carbon accumulation in cotton production systems in the Brazilian cerrado. *Acta Sci. Agron.* 42.
- Ghimire, R., Machado, S., Rhinhart, K., 2015. Long-term crop residue and nitrogen management effects on soil profile carbon and nitrogen in wheat-fallow systems. *Agron. J.* 107, 2230–2240.
- Gurung, R.B., Ogle, Stephen M., Breidt, F. Jay, Williams, Stephen A., Parton, William J., 2020. Bayesian calibration of the DayCent ecosystem model to simulate soil organic carbon dynamics and reduce model uncertainty. *Geoderma* 376 (2020), 114529.
- Halvorson, A., Reule, C., 2007. How to enhance soil organic carbon sequestration. *Fluid Journal* 17–19. <https://fluidfertilizer.org/wp-content/uploads/2016/05/57P17-19.pdf>.
- Halvorson, A.D., Schlegel, A.J., 2012. Crop rotation effect on soil carbon and nitrogen stocks under limited irrigation. *Agron. J.* 104, 1265–1273.
- Halvorson, A.D., Wienhold, B.J., Black, A.L., 2002. Tillage, nitrogen, and cropping system effects on soil carbon sequestration. *Soil Sci. Soc. Am. J.* 66, 906–912.
- Halvorson, A.D., Follett, R.F., Reule, C.A., Del Grosso, S., 2009. Soil organic carbon and nitrogen sequestration in irrigated cropping systems of the Central Great Plains. In: Lal, R., Follett, R.F. (Eds.), *Soil Carbon Sequestration and the Greenhouse Effect - SSSA Special Publication*. Wiley, pp. 141–157.
- Hammerberg, A.L., Stetson, S.J., Osborne, S.L., Schumacher, T.E., Pikul Jr., J.L., 2012. Corn residue removal impact on soil aggregates in a No-till corn/soybean rotation. *Soil Sci. Soc. Am. J.* 76 (4), 1390–1398.
- Hao, X., Chang, C., Travis, G.R., Zhang, F., 2003. Soil carbon and nitrogen response to 25 annual cattle manure applications. *J. Plant Nutr. Soil Sci.* 166 (2), 239–245. <https://doi.org/10.1002/jpln.200390035>.
- Harmel, R.D., Cooper, R.J., Slade, R.M., Haney, R.L., Arnold, J.G., 2006. Cumulative uncertainty in measured streamflow and water quality data for small watersheds. *Transactions of the Asabe* 49 (3), 689–701.
- Hartman, M.D., William, W.J., Del Grosso, S.J., Easter, M., et al., 2021. *The Daily Century Ecosystem, Soil Organic Matter, Nutrient Cycling, Nitrogen Trace Gas, and Methane Model. User Manual, Scientific Basis, and Technical Documentation*. Natural Resource Ecology Laboratory Colorado State University, Fort Collins, Colorado.
- Helton, J.C., Davis, F.J., 2003. Latin hypercube sampling and the propagation of uncertainty in analyses of complex systems. *Reliab. Eng. Syst. Saf.* 81 (1), 23–69.
- Hulugalle, N.R., Weaver, T.B., Finlay, L.A., Heimoana, V., 2013. Soil organic carbon concentrations and storage in irrigated cotton cropping systems sown on permanent beds in a Vertosol with restricted subsoil drainage. *Crop Pasture Sci.* 64, 799–805.
- Ismail, I., Blevins, R.L., Frye, W.W., 1994. Long-Term no-tillage effects on soil properties and continuous corn yields. *Soil Sci. Soc. Am. J.* 58, 193–198. <https://doi-org.libprox.y.unl.edu/10.2136/sssaj1994.03615995005800010028x>.
- Izaurrealde, R.C., Mcgill, W.B., Williams, J.R., 2012. *Development and application of the EPIC model for carbon cycle, greenhouse-gas, mitigation and biofuel studies*. <https://doi.org/10.1016/B978-0-12-386897-8.00017-6>. ISBN: 9780123868978.
- Jarecki, M.K., Lal, R., 2005. Soil organic carbon sequestration rates in two long-term no-till experiments in Ohio. *Soil Sci. Soc. Am. J.* 58, 280–291.
- Jin, V.L., Varvel, G., 2018. All; 2001–2016. Ver. GPSR NATRES. USDA-ARS Natural Resources Database. Project, Fort Collins, CO. NEMEIRR. <https://gpsr.ars.usda.gov/NEMEIRR>.
- Jin, V.L., Schmer, M.R., Wienhold, B.J., Stewart, C.E., Varvel, G.E., Sindelar, A.J., Follett, R.F., Mitchell, R.B., Vogel, K.P., 2015. Twelve years of stover removal increases soil erosion potential without impacting yield. *Soil Sci. Soc. Am. J.* 79, 1169–1178.
- Kong, A.Y.Y., Six, J., Bryant, D.C., Denison, R.F., van Kessel, C., 2005. The relationship between carbon input, aggregation, and soil organic carbon stabilization in sustainable cropping systems. *Soil Sci. Soc. Am. J.* 69, 1078–1085.
- Li, C., Aber, J., Stange, F., Butterbach-Bahl, K., Papen, H., 2000. A process-oriented model of N₂O and NO emissions from forest soils: 1. Model development. *J. Geophys. Res.* 105, 4369e4384.
- Luo, Y., Ahlström, A., Allison, S.D., Batjes, N.H., Brovkin, V., Carvalhais, N., Chappell, A., Ciais, P., Davidson, E.A., Finzi, A., 2016. Toward more realistic projections of soil carbon dynamics by Earth system models. *Global Biogeochem. Cycles* 30, 40–56.
- Mathers, C., Black, C.K., Segal, B.D., Gurung, R.B., Zhang, Y., Easter, M.J., Williams, S., Motew, M., Campbell, E.E., Brummitt, C.D., Paustian, K., Kumar, A.A., 2023. Validating DayCent-CR for cropland soil carbon offset reporting at a national scale. *Geoderma* 438, 116647.
- Mitchell, J.P., Shrestha, A., Horwath, W.R., Southard, R.J., Madden, N., Veenstra, J., Munk, D.S., 2015. Tillage and cover cropping affect crop yields and soil carbon in the San Joaquin valley, California. *Agron. J.* 107, 588–596.
- Mitchell, J.P., Shrestha, A., Mathesius, K., Scow, K.M., Southard, R.J., Haney, R.L., Schmidt, R., Munk, D.S., Horwath, W.R., 2017. Cover cropping and no-tillage improve soil health in an arid irrigated cropping system in California's San Joaquin Valley, USA. *Soil Tillage Res.* 165, 325–335.
- Monreal, C.M., Janzen, H.H., 1993. Soil organic-carbon dynamics after 80 years of cropping a Dark Brown Chernozem. *Can. J. Soil Sci.* 73, 133–136.
- Ogle, S.M., Breidt, F.J., Easter, M., et al., 2007. An empirically based approach for estimating uncertainty associated with modelling carbon sequestration in soils. *Ecol. Model.* 205, 453–463. <https://doi.org/10.1016/j.ecolmodel.2007.03.007>.
- Ogle, S.M., Breidt, F.J., Easter, M., et al., 2010. Scale and uncertainty in modeled soil organic carbon stock changes for US croplands using a process-based model. *Global Change Biol.* 16, 810–822. <https://doi.org/10.1111/j.1365-2486.2009.01951.x>.
- Olson, K.R., Ebelhar, S.A., Lang, J.M., 2010. Cover crop effects on crop yields and soil organic carbon content. *Soil Sci.* 175, 89–98.
- Parton, W.J., Holland, E.A., Del Grosso, S.J., Hartman, M.D., Martin, R.E., Mosier, A.R., Ojima, D.S., Schimel, D.S., 2001. Generalized model for NO_x and N₂O emissions

- from soils. *J. Geophys. Res.: Atmosph.* 106, 17403–17419. <https://doi.org/10.1029/2001JD900101>.
- Parton, W.J., Ojima, D.S., Cole, C.V., Schimel, D.S., 1994. A General Model for Soil Organic Matter Dynamics - Sensitivity to Litter Chemistry, Texture and Management. In: Bryant, R.B., Arnold, R.W. (Eds.), *Quantitative Modeling of Soil Forming Processes*, pp. 147–167.
- Pimentel, D., Hepperly, P., Hanson, J., Douds, D., Seidel, R., 2005. Environmental, energetic, and economic comparisons of organic and conventional farming systems. *Bioscience* 5, 573–582.
- Powers, W., Auvermann, B., Cole, N., Gooch, C., Grant, R., Hatfield, J., Hunt, P., Johnson, K., Leytem, A., Liao, W., Powell, J., 2014. Quantifying greenhouse gas sources and sinks in animal production systems. In: Eve, M. (Ed.), *Quantifying Greenhouse Gas Fluxes in Agriculture and Forestry: Methods for Entity-Scale Inventory*. U.S. Department of Agriculture et al. USDA Technical Bulletin 1939.
- Rafique, R., Kumar, S., Luo, Y., Xu, X., Li, D., Zhang, W., Asam, Z.-u.-Z., 2014. Estimation of greenhouse gases (N₂O, CH₄ and CO₂) from no-till cropland under increased temperature and altered precipitation regime: a DAYCENT model approach. *Global Planet. Change* 118, 106–114.
- Rasmussen, P.E., Smiley, R.W., 1997. Soil carbon and nitrogen change in long-term agricultural experiments at Pendleton, Oregon. In: Paul, E.A., Paustian, K., Elliot, E. T., Cole, C.V. (Eds.), *Soil Organic Matter in Temperate Agroecosystems - Long Term Experiments in North America*. CRC Press, pp. 353–360.
- Rochester, L.J., 2011. Sequestering carbon in minimum-tilled clay soils used for irrigated cotton and grain production. *Soil Tillage Res.* 112, 1–7.
- Rothamsted, Research., 2018. Broadbalk soil organic carbon content 1843-2015. *Electronic Rothamsted Archive*. Rothamsted Research. <https://doi.org/10.23637/KeyRefOABKsoc-02>.
- Sainju, U.M., Whitehead, W.F., Singh, B.P., 2005. Carbon accumulation in cotton, sorghum, and underlying soil as influenced by tillage, cover crops, and nitrogen fertilization. *Plant Soil* 273, 219–234.
- Saltelli, A., Tarantola, S., Campolongo, F., 2000. Sensitivity analysis as an ingredient of modeling. *Stat. Sci.* 15 (4), 377–395.
- Saltelli, A., Annoni, P., Azzini, I., Campolongo, F., Ratto, M., Tarantola, S., 2010. Variance based sensitivity analysis of model output. Design and estimator for the total sensitivity index. *Comput. Phys. Commun.* 181 (2), 259–270.
- Senapati, N., Hulugalle, N.R., Smith, P., Wilson, B.R., Yeluripati, J.B., Daniel, H., Ghosh, S., Lockwood, P., 2014. Modelling soil organic carbon storage with RothC in irrigated Vertisols under cotton cropping systems in the sub-tropics. *Soil Tillage Res.* 143, 38–49.
- Shoaib, S.A., Khan, M.Z.K., Sultana, N., Mahmood, T.H., 2021. Quantifying uncertainty in food security modeling. *Agriculture* 11 (1), 33.
- Sobol, I.M., 2001. Global sensitivity indices for nonlinear mathematical models and their Monte Carlo estimates. *Math. Comput. Simulat.* 55 (1), 271–280.
- Thornton, M., Shrestha, R., Wei, Y., Thornton, P.E., Kao, S., 2020. Daymet: Daily SurfSWF Weather Data on a 1-km Grid for North America; Version 4, ORNL DASWF. Oak Ridge, Tennessee.
- Tolson, B.A., Shoemaker, C.A., 2007. Dynamically dimensioned search algorithm for computationally efficient watershed model calibration. *Water Resour. Res.* 43 (1), W01413.
- USEPA, 2020. Inventory of U.S. Greenhouse Gas Emissions and Sinks: 1990–2018, 1200 Pennsylvania Ave., NW, Washington DC. <http://www.epa.gov/ghgemissions/inventory-us-greenhouse-gas-emissions-and-sinks-1990-2018> (Accessed 12 October 2022).
- Varvel, G.E., 2006. Soil organic carbon changes in diversified rotations of the western corn belt. *Soil Sci. Soc. Am. J.* 70, 426–433.
- Veenstra, J.J., Horwath, W.R., Mitchell, J.P., Munk, D.S., 2006. Conservation tillage and cover cropping influence soil properties in San Joaquin Valley cotton-tomato crop. *Calif. Agric.* 60, 146–153. https://escholarship.org/content/qt38t4n0r5/qt38t4n0r5_noSplash_516a33a25e05de7e88ace3584e02d446.pdf?t=krnosa.
- Vrugt, J.A., ter Braak, C.J.F., Clark, M.P., Hyman, J.M., Robinson, B.A., 2008. Treatment of input uncertainty in hydrologic modeling: doing hydrology backward with Markov chain Monte Carlo simulation: forcing data error using MCMC sampling. *Water Resour. Res.* 44.
- Vrugt, J.A., ter Braak, C.J.F., Diks, C.G.H., Robinson, B.A., Hyman, J.M., Higdon, D., 2009. Accelerating Markov chain Monte Carlo simulation by differential evolution with self-adaptive randomized Subspace sampling. *Int. J. Nonlinear Sci. Numer. Stimul.* 10.
- Wang, X., He, X., Williams, J.R., Izaurralde, R.C., Atwood, J.D., 2005. Sensitivity and uncertainty analysis of crop yields and soil organic carbon simulation with EPIC. *Transactions of the ASAE* 48 (3), 1041–1054.
- Wang, X., Potter, S.R., Williams, J.R., Atwood, J.D., Pitts, T., 2006. Sensitivity analysis of APEX for national assessment. *Transactions of the ASAE* 49 (3), 679–688.
- Wang, X., Williams, J.R., Gassman, P.W., Baffaut, C., Izaurralde, R.C., Jeong, J., Kiriny, J. R., 2012. EPIC and APEX: model use, calibration, and validation. *Transactions of the ASAE* 55 (4), 1447–1462.
- Wang, X., Yen, H., Liu, Q., Liu, J., 2014. An auto-calibration tool for the Agricultural Policy Environmental eXtender (APEX) model. *Trans. ASABE (Am. Soc. Agric. Biol. Eng.)* 57 (4), 1087–1098. <https://doi.org/10.13031/trans.57.10601>.
- Wegner, B.R., Chalise, K.S., Singh, S., Lai, L., Abagandura, G.O., Kumar, S., Osborne, S.L., Lehman, R.M., Jagadamma, S., 2018. Response of soil surface greenhouse gas fluxes to crop residue removal and cover crops under a corn-soybean rotation. *J. Environ. Qual.* 47, 1146–1154.
- Wiesmeier, M., Urbanski, L., Hobbey, E., Lang, B., von Lützw, M., Marin-Spiotta, E., van Wesemael, B., Rabot, E., Lieb, M., Garcia-Franco, N., Wollschläger, U., Vogel, H.-J., Kögel-Knabner, I., 2019. Soil organic carbon storage as a key function of soils – a review of drivers and indicators at various scales. *Geoderma* 333, 149–162.
- Williams, J.R., 1995. The EPIC model. In: Singh, V.P. (Ed.), *Computer Models Of Watershed Hydrology*, 909-1000, Highlands Ranch, Colo. Water Resources Publications.
- Williams, J.R., Izaurralde, R.C., 2006. The APEX model. In: Singh, V.P., Frevert, D.K. (Eds.), *Watershed Models*. CRC Press, Boca Raton, Fla, pp. 437–482.
- Wutzler, T., Reichstein, M., 2007. Soils apart from equilibrium – consequences for soil carbon balance modelling. *Biogeosciences* 4, 125–136.
- Yen, H., Wang, X., Fontane, D.G., Harmel, R.D., Arabi, M., 2014. A Framework for Propagation of Uncertainty Contributed by Parameterization, Input Data, Model Structure, and Calibration/validation Data in Watershed Modeling, vol. 54, pp. 211–221.
- Yen, H., Jeong, J., Wang, X., Lu, S., Kim, M.K., Su, Y.W., 2015. Assessment of model configuration effect by alternative evapotranspiration, runoff, and water routing functions on watershed modeling using SWAT. *Transactions of the ASABE* 58 (2), 393–404.
- Yen, H., Jeong, J., Smith, D.R., 2016. Evaluation of dynamically dimensioned search algorithm for optimizing SWAT by altering sampling distributions and searching range. *J. Am. Water Resour. Assoc.* 52 (2), 443–455.
- Zhang, X., Izaurralde, R.C., Arnold, J.G., Williams, J.R., Srinivasan, R., 2013. Modifying the Soil and Water Assessment Tool to simulate cropland carbon flux: model development and initial evaluation. *Sci. Total Environ.* 463–464, 810–822.